







Measurement of the thermal neutron capture cross section by ^9Be using the neutron flux from a nuclear research reactor and the AMS technique

D. J. Marín-Lámbarri ^{1,*}, J. García-Ramírez ¹, E. Sánchez-Zúñiga,¹ S. Padilla,¹ L. Acosta ¹, E. Chávez ¹,
H. S. Cruz-Galindo ², A. Huerta,¹ G. Méndez,^{1,3} R. Raya-Arredondo,² M. Rodríguez-Ceja,^{1,4}
C. Solís,¹ and L. Barrón-Palos ¹

¹*Instituto de Física, Universidad Nacional Autónoma de México, Apartado Postal 20-364, 01000 Ciudad de México, México*

²*Instituto Nacional de Investigaciones Nucleares, Carretera México-Toluca, Km. 36.5, La Marquesa, 52750 Ocoyoacac, México, México*

³*CONACYT, Instituto de Física, Universidad Nacional Autónoma de México, Apartado Postal 20-364, 01000 Ciudad de México, México*

⁴*Facultad de Ciencias, Universidad Nacional Autónoma de México, Circuito de la Investigación Científica S/N, Ciudad Universitaria, 04510 Ciudad de México, México*



(Received 13 May 2020; revised 29 July 2020; accepted 3 September 2020; published 2 October 2020)

We report on the measurement of the thermal neutron capture cross section by ^9Be , using ^{14}N as a benchmark for the development of our protocol, which implies the combination of two precise techniques: neutron activation in a nuclear research reactor and accelerator mass spectrometry (AMS). Beryllium oxide (BeO), graphite, and uracil ($\text{C}_4\text{H}_4\text{N}_2\text{O}_2$) samples were irradiated at the TRIGA MARK III nuclear research reactor facility at Instituto Nacional de Investigaciones Nucleares (ININ), México. Later on, isotopic concentrations were quantified by AMS at Laboratorio de Espectrometría de Masas con Aceleradores (LEMA) of the Instituto de Física, Universidad Nacional Autónoma de México (IF-UNAM), Mexico. Cross sections for the $^9\text{Be}(n, \gamma)^{10}\text{Be}$ and $^{14}\text{N}(n, p)^{14}\text{C}$ nuclear reactions were extracted for thermal neutrons.

DOI: [10.1103/PhysRevC.102.044601](https://doi.org/10.1103/PhysRevC.102.044601)

I. INTRODUCTION

The reason for the existence of Laboratorio de Espectrometría de Masas con Aceleradores (LEMA) at the Instituto de Física, Universidad Nacional Autónoma de México (IF-UNAM) is the precise measurement of radioactive isotope concentrations for interdisciplinary applications [1–3]. The availability of standard materials, those with precisely known ratio of the rare (radioactive) to stable isotope, is of paramount importance. We considered it worth trying to produce beryllium standards by enriching common BeO in ^{10}Be by controlled neutron irradiation. The abundant use of beryllium in nuclear reactors and material development in the industry (see, e.g., Refs. [4,5]) highlights the importance in the precise determination of the thermal neutron capture cross section as well. Looking up in the literature the value of the thermal neutron capture cross section by ^9Be , we found that it had been indirectly measured and calculated by different methods, but there is not a general agreement about its precise value [4,5]. So we decided to solve the puzzle by measuring it directly using two of the largest Mexican nuclear facilities: a nuclear research reactor and an accelerator mass spectrometry laboratory.

Knowing the precise values of neutron capture cross sections is also important to understand both stellar and primordial nucleosynthesis [6–8]. A well known example in

stellar nucleosynthesis is the s and r processes that are responsible for the production of about half of the elements heavier than iron. In light nuclei, the role of the beryllium isotopes (^9Be and ^{10}Be) in the synthesis of heavier elements is considered of minor importance but still not fully understood [9]. Especially the $^9\text{Be}(n, \gamma)^{10}\text{Be}$ reaction for low energy (thermal and epithermal) neutrons has not been measured, and it is needed beyond models and calculations, to complete the picture of the primordial and star synthesis of light elements. In the literature, it is possible to find previous studies of these reactions [7,10–20]. However, most of these publications deal with higher neutron energies (from 25 keV and up to 14 MeV).

The $^{14}\text{N}(n, p)^{14}\text{C}$ reaction has a capture cross section for thermal neutrons that is very large, so much that it stands as the most important neutron poison in stellar nucleosynthesis. It has been measured with great accuracy [21,22] and therefore it can be used as a benchmark to validate our experimental protocol for the study of the $^9\text{Be}(n, \gamma)^{10}\text{B}$ reaction. As it will become clear when we describe our measurements, it seemed possible for us to be able also to measure simultaneously the $^{13}\text{C}(n, \gamma)^{14}\text{C}$ nuclear reaction of importance in the s process [23–26].

II. EXPERIMENTAL METHOD

Three different stages were involved: sample preparation, neutron irradiation, and the accelerator mass spectrometry (AMS) analysis.

*marinlambarri@gmail.com

A. Sample preparation

Beryllium oxide. BeO samples were prepared (proxy 8 mg of Be each) from 8 ml of Be standard solution [Beryllium ICP Standard Solution, $\text{Be}_4\text{O}(\text{C}_2\text{H}_3\text{O}_2)_6$, 1000 mg/1 Be Merck], which is currently used as carrier and blank in AMS. To extract BeO, ammonia was added to the solution and BeOH was precipitated. This precipitate was separated by centrifugation and the solid was dried and finally calcined at 1000 °C for one hour in a ceramic crucible, resulting in pure BeO. Three samples were placed into polyethylene containers for neutron irradiation. An additional sample was not irradiated and kept as reference.

Graphite and uracil. As mentioned above, to test our protocols we studied the $^{14}\text{N}(n, p)^{14}\text{C}$ reaction. In this case we used uracil ($\text{C}_4\text{H}_4\text{N}_2\text{O}_2$). In the attempt to measure the $^{13}\text{C}(n, \gamma)^{14}\text{C}$ reaction cross section, we used natural graphite (98.9% of ^{12}C and 1.1% of ^{13}C). In the first case, uracil powder was enclosed in two polyethylene containers. In the second case, samples were prepared from natural graphite powder. The powder was enclosed in a principal quartz heat-sealed container, followed by a second aluminum container; these containers are used when samples are required to be exposed to high neutron fluxes for extended periods of time (see Sec. II B). Also blank (not irradiated) samples were prepared for both materials.

B. Neutron irradiation

The irradiation times and stations for each sample were chosen according to the reported thermal neutron cross-sections for the nuclei of interest [27] and the rare-to-stable isotope ratio that we wanted to achieve in order to have a sensible determination of the cross sections.

The 1 MW TRIGA MARK III reactor at Instituto Nacional de Investigaciones Nucleares (ININ) in Mexico, is a pool-type research reactor with a movable core, cooled and moderated with light water. The core is surrounded by water at room temperature so neutrons are moderated following a Maxwell-Boltzmann energy distribution, with the maximum at 25 meV for a temperature of 290 K; these neutrons are known as thermal neutrons. The structure of the core is a circular arrangement of fuel, control rods, and graphite elements. Thermal neutron fluxes of up to $3.3 \times 10^{13} \text{ n/cm}^2\text{s}$ can be reached in stationary mode. The fuel elements are distributed in five concentric circles known as rings (labeled A, B, C, D, and F), around a central irradiation station (A1), also called the central thimble (Fig. 1). There is a sixth ring, occupied by graphite elements (reflectors) and two irradiation stations; one of them is known as SINCA (Pneumatic Capsule-Irradiation System). SIRCA (Rotary Capsule-Irradiation System), is the outermost irradiation station. This station rotates continuously around the reactor core, outside of the graphite reflectors and the metallic container; this is the reason why the neutron flux at this position is a factor of 2 lower than that at SINCA.

The energy spectrum of the neutrons at the SIRCA station is predominantly thermal, with a flux of $2.6 \times 10^{12} \text{ n/cm}^2\text{s}$ and a weak epithermal flux of $2.26 \times 10^{11} \text{ n/cm}^2\text{s}$, which is the lowest neutron flux we used for any sample. The thermal neutron flux at the SINCA station is $4.42 \times 10^{12} \text{ n/cm}^2\text{s}$, five

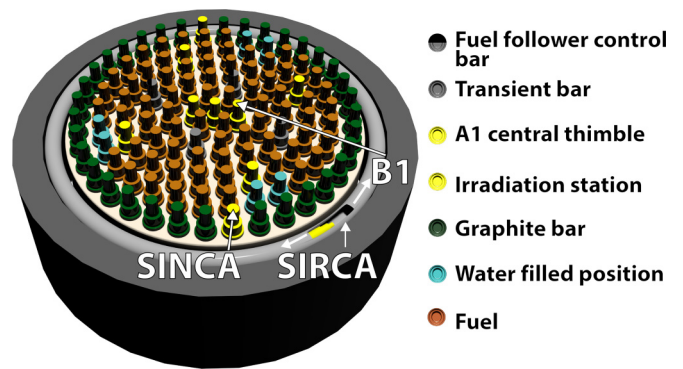


FIG. 1. Schematic representation of the TRIGA-MARK-III nuclear research reactor core. The different irradiation stations used in this work are labeled. B1 is the one closer to the center and with the highest neutron flux. The SINCA irradiation station is in the sixth ring. SIRCA, the moving irradiation station, is represented by an arrow.

times smaller than that at the position in the central thimble [28–30]. SIRCA was used for the neutron irradiation of the BeO samples, two irradiated for 30 minutes and a third one irradiated for 120 minutes. Uracil samples were irradiated for 20 seconds in the SINCA system. In the second ring (B), the thermal neutron flux is $2.3 \times 10^{13} \text{ n/cm}^2\text{s}$ and B1 (see Fig. 1) was used for the neutron irradiation of the graphite samples: Two samples were irradiated for 10 hours and a second set of three samples, inside a cadmium container, were irradiated for 2 hours. Cadmium absorbs neutrons with energies below 0.5 eV, therefore by enclosing the sample in such a container it is possible to verify that the contribution of fast neutrons to the measured cross sections was negligible (see Sec. III).

C. AMS analysis

To quantify the ^{10}Be and ^{14}C in the $^9\text{Be}(n, \gamma)$, $^{13}\text{C}(n, \gamma)$, and $^{14}\text{N}(n, p)$ nuclear reactions, the accelerator mass spectrometry (AMS) technique was used, taking advantage of the LEMA facility at IF-UNAM. A detailed description of this facility can be found at [1] and its upgraded configuration in [2] (see Fig. 2).



FIG. 2. LEMA at IF-UNAM, where AMS analysis were performed.

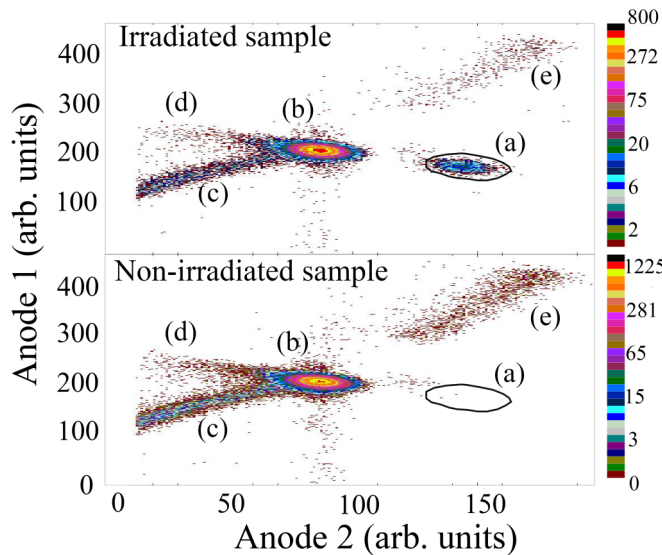


FIG. 3. The top spectrum corresponds to an irradiated sample, while the bottom one corresponds to a nonirradiated one. Rare isotopes, in this case ^{10}Be , are counted one by one in a split-anode ionization chamber. A two-dimensional plot, where the pulse height signals from each anode are plotted against each other, allows particle identification by the $E-\Delta E$ technique. In this plot ^{10}Be counts will lie in the region of interest (ROI) labeled as (a). The events from the stable isobar ^{10}B will correspond to the locus labeled (b). Loci (c), (d), and (e) correspond to high count-rate response of the detector. The excess of ^{10}Be produced by neutron irradiation is evident.

The $^{14}\text{C}/^{12}\text{C}$ ratio is routinely extracted for each unknown sample through 225 independent measurements arranged in 15 sets of 15. Each measurement lasts for 30 s. In each measurement a number of ^{12}C , ^{13}C , and ^{14}C ions is counted and compared with an identical measurement of a sample with known concentration of all carbon isotopes (typically an OXA-II standard). The statistical treatment of the data follows the accepted formulation by the AMS community [3].

This technique offers a complementary tool to measure cross sections of nuclear reactions. The list of reaction products of interest in astrophysics includes radioisotopes over the entire mass range, e.g., ^{10}Be , ^{14}C , ^{26}Al , ^{129}I , and a number of actinide isotopes including ^{244}Pu .

Beryllium. For the measurement of the $^{10}\text{Be}/^9\text{Be}$ isotopic ratio after irradiation, five aliquots were taken from each sample, mixed with niobium and pressed in the cathodes used in the Sputter Negative Ion Cesium Source (SNICS) of LEMA's isotope separator for AMS analysis. To identify and count the number of ^{10}Be ions in the split-anode ionization chamber ($E-\Delta E$ isobutane gas), two-dimensional $E-\Delta E$ plots are generated as in the example shown in Fig. 3. In the top panel, data are shown for the nonirradiated material, where only a few counts are identified as ^{10}Be in the expected region of interest (ROI, dark region). In contrast, when an irradiated sample is measured, many counts appear within the ^{10}Be ROI, as shown at the bottom of Fig. 3. In these maps, it is clear that the identification of the mass-10 isobars (^{10}Be and ^{10}B), and therefore the $^{10}\text{Be}/^9\text{Be}$ ratio, can be obtained using the number of ^9Be ions from the charge integration in a Faraday

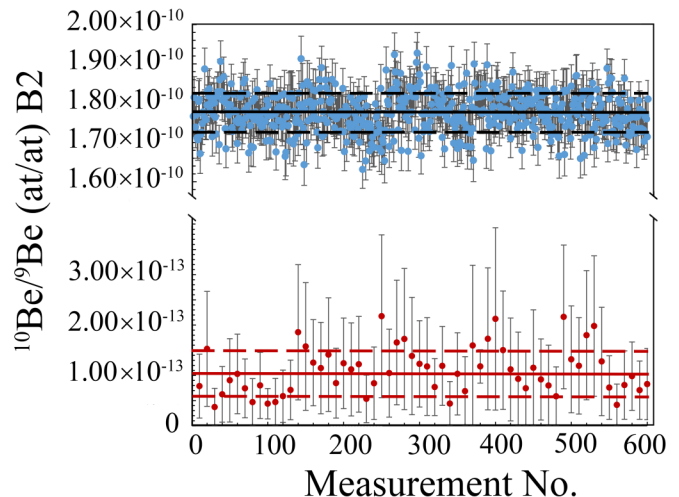


FIG. 4. Data from irradiated (blue dots) and non-irradiated (red dots, averaged over ten values) samples. Note the three orders of magnitude between blue and red dots. The continuous and dashed lines show the average and the standard deviation, respectively.

cup. The rare to stable isotope ratio is obtained averaging 12 sets of 10 measurements of 30 s length for each cathode. As five aliquots were taken, a total of 600 measurements were carried out for each sample. Measurements were performed with the charge state 1^+ for both masses (9 and 10) after the accelerator and also after the passive absorber. After the high energy magnet, typical currents for $^9\text{Be}^+$ were $1\ \mu\text{A}$ with a beam energy of 1.40 MeV. All measured $^{10}\text{Be}/^9\text{Be}$ ratios were normalized to a 01-5-1 standard sample with a nominal value of $(2.709 \pm 0.029) \times 10^{-11}$ [31].

For each cathode, the $^{10}\text{Be}/^9\text{Be}$ ratio was obtained. Figure 4 shows 600 values for an irradiated sample compared with those of the nonirradiated one (B0), several orders of magnitude smaller. Table I shows the average for each sample with their corresponding uncertainties used for the calculation of the $^9\text{Be}(n, \gamma)^{10}\text{Be}$ reaction cross section.

In this table, a relation between the irradiation time and the $R_{^{10}\text{Be}/^9\text{Be}}$ ratio is evident. The ^{10}Be concentration in the nonirradiated sample B0 shows the quality of both the Be sample preparation in the laboratory and the measurement by the AMS technique. B1 and B3 samples were irradiated the same period of time, 30 minutes, while B2 was irradiated for 120 minutes.

TABLE I. Average of the $R_{^{10}\text{Be}/^9\text{Be}}$ ratio for the three irradiated samples (B1 and B3 for 30 minutes and B2 for 120 minutes, all with a thermal neutron flux of $2.6 \times 10^{12}\ \text{n}/\text{cm}^2\ \text{s}$), and the nonirradiated sample B0.

Sample	Irradiation time (s)	$R_{^{10}\text{Be}/^9\text{Be}}$ (10^{-14})	1σ (10^{-14})
B0	0	4.64	0.45
B1	1800	4 530	50
B2	7200	17 757	190
B3	1800	4 652	50

TABLE II. Average of the $^{14}\text{C}/^{12}\text{C}$ ratio for the uracil and graphite samples. Uracil samples (U1 and U2) were irradiated at SINCA ($4.42 \times 10^{12} \text{ n/cm}^2\text{s}$), while graphite samples (G1, G2, G3, G1c, G2c, and G3c) were irradiated at the B1 irradiation station ($2.3 \times 10^{13} \text{ n/cm}^2\text{s}$).

Sample	Irradiation time (s)	$R_{^{14}\text{C}/^{12}\text{C}}$ (10^{-15})	1σ (10^{-15})
G0	0	8.72	6.31
U0	0	10.30	2.05
U01	0	13	2.56
U1	20	117 000	567
U2	20	121 000	538
G1	36 000	1 460 000	3780
G2	36 000	1 450 000	3610
G1c	7 200	6 190	46.80
G2c	7 200	6 190	66.40
G3c	7 200	6 070	435

The Berillium isotopic ratios were normalized to a standard material using the equation

$$R_{^{10}\text{Be}/^9\text{Be}} = \frac{R_s R_{nstd}}{R_{mstd}}, \quad (1)$$

where $R_{^{10}\text{Be}/^9\text{Be}}$ is the normalized isotopic ratio of the sample, R_s and R_{nstd} are the raw isotopic ratios for both sample and standard measured by AMS, and R_{mstd} is the nominal value of the isotopic ratio of the standard used in the measurement.

To calculate the uncertainty of the normalized isotopic ratio ($R_{^{10}\text{Be}/^9\text{Be}}$) we have to take into account three sources: R_s , R_{nstd} , and R_{mstd} . For R_s and R_{mstd} , we take the maximum between the standard deviation of the total number of beryllium isotopes detected and that of the distribution of the 600 measurements. The uncertainty of R_{nstd} is supplied by Nishiizumi [31]. Finally, the uncertainty of normalized isotopic ratio ($R_{^{10}\text{Be}/^9\text{Be}}$) is calculated through the standard error-propagation method.

Carbon. For the reactions producing ^{14}C , cathodes were prepared directly from graphite and uracil, respectively, without adding any other material. There were three nonirradiated cathodes (one graphite and two uracil) and seven irradiated (five graphite and two uracil, three of the last corresponding to samples irradiated inside a cadmium container). The $^{14}\text{C}/^{12}\text{C}$ ratio measured in each sample is presented in Table II. It is important to point out that no standard was used for normalization in the case of graphite and uracil, therefore $R_{^{14}\text{C}/^{12}\text{C}} = R_s$.

The $R_{^{13}\text{C}/^{12}\text{C}}$ was also determined in all samples, resulting in a value of $0.01 \pm 1.7 \times 10^{-5}$ for both graphite and uracil, independently of whether the samples had been irradiated or not. The $^{12}\text{C}(n, \gamma)^{13}\text{C}$ reaction has a very small cross section, $3.53 \pm \text{NA mb}$ at thermal neutron energies [27], therefore variations in the relative concentration between ^{13}C and ^{12}C are negligible for the irradiation times and neutron fluxes used in this work.

In Fig. 5 we show the contrast between the measurements of irradiated (right) to nonirradiated samples (left) for both graphite (top row) and uracil (bottom row).

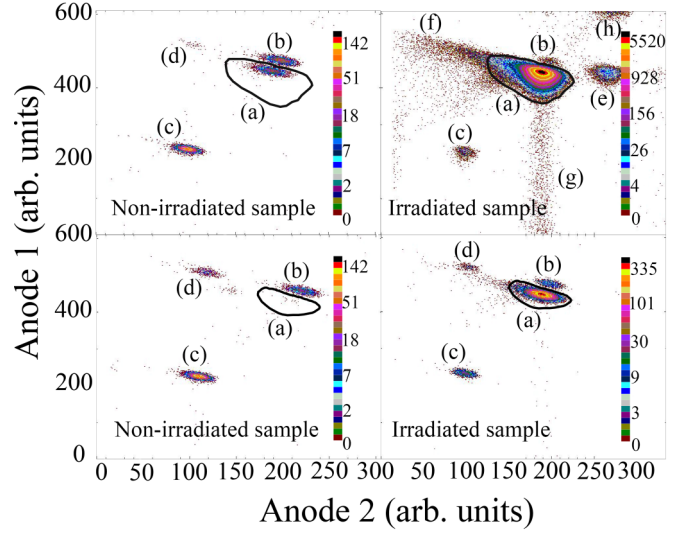


FIG. 5. Similar to Fig. 3, here we show four two-dimensional $E-\Delta E$ spectra for the carbon measurements. The left column shows data from the nonirradiated samples and in the right column irradiated samples are shown; uracil on top and graphite on bottom. In every spectrum, the ^{14}C ROI is labeled as (a). The simultaneous detection of two ^7Li produces signals in the locus labeled as (b) and (c) corresponds to the detection of just one ^7Li ion. Unidentified molecular contamination produces counts in (d). The loci (e), (f), (g), and (h) appear as a detector response to high count rate.

III. CROSS SECTIONS

At any given time, the fractional rate of change of an isotope being produced by a thermal-neutron-induced nuclear reaction [(n, γ) or (n, p) in our case] is given by

$$\frac{dN_{\text{rare}}}{dt} = N_{\text{target}} \sigma_n \phi_n, \quad (2)$$

where we use the labels “rare” for the isotope being produced in the reaction (^{10}Be or ^{14}C) and “target” for the target isotope (^9Be , ^{13}C , or ^{14}N). $N_{\text{rare/target}}$ is the number of rare/target isotopes present in the sample at time t , σ_n is the cross section for the nuclear reaction at thermal neutron energy (E_{th}), and ϕ_n is the neutron flux incident on the sample. The target isotope decreases in time with the same rate that the rare isotope increases, so its number at any given time is

$$N_{\text{target}} = N_{\text{target}}^0 \exp(-\sigma_n \phi_n t). \quad (3)$$

The superscript 0 indicates the number of target nuclei at irradiation time $t = 0$. Using Eq. (3) to solve Eq. (2), and identifying by the label “stable” the isotope with respect to which the rare isotope is measured (^{12}C or ^9Be) so that $N_{\text{rare}}/N_{\text{stable}} = R_{\text{rare/stable}}$, we obtain

$$\sigma_n(E_{\text{th}}) = -\frac{1}{\phi_n t_i} \ln \left[1 - \left(\frac{R_{\text{rare/stable}} - R_{\text{rare/stable}}^0}{R_{\text{target/stable}}^0} \right) \right], \quad (4)$$

with t_i the irradiation time. For the $^{14}\text{N}(n, p)^{14}\text{C}$ and $^{13}\text{C}(n, \gamma)^{14}\text{C}$ reactions, the target isotopes are ^{14}N and ^{13}C respectively, while ^{12}C is the stable isotope. For the $^9\text{Be}(n, \gamma)^{10}\text{Be}$ reaction, target and stable isotope are the same, therefore $R_{\text{target/stable}}^0 = 1$.

$^{14}\text{N}(n, p)^{14}\text{C}$. In this case, the ratio of ^{14}N to ^{12}C before irradiation is required [see Eq. (4)]. The concentration of ^{14}N is not determined via AMS; however, it is directly correlated with the number of ^{12}C atoms via the stoichiometry of the uracil compound $\text{C}_4\text{H}_4\text{N}_2\text{O}_2$ and the natural abundance of both isotopes. We know that the abundance of the ^{12}C isotope is 98.9%, and 99.34% of nitrogen is ^{14}N [23]; considering this relation it is possible to calculate the ratio of interest, $R_{^{14}\text{N}/^{12}\text{C}}^0 \simeq 0.50$.

The cross section at thermal neutron energies, in this case, results in 2.07 ± 0.37 b. This result is in agreement with the value of 1.91 b previously reported for this reaction [27]. Previous measurements [21,22] report values of 1.93 ± 0.05 b and 1.86 ± 0.03 b, respectively. It is important to mention that the main factor of uncertainty in our measurement comes from the irradiation time using the pneumatic system SINCA at the ININ research reactor, where it takes approximately 6 s for the sample to arrive at the irradiation station and it is uncertain in which portion of their travel the samples are already “seeing” neutrons; this transport time is significant compared to the total irradiation time of the samples (20 s). The other cross sections discussed in this work do not suffer from this large uncertainty in the irradiation time, since other positions at the reactor were used and irradiation times are much longer.

$^9\text{Be}(n, \gamma)^{10}\text{Be}$. From Eq. (4), a cross section value for the thermal neutron capture in ^9Be results in 9.7 ± 0.53 mb.

Considering that this is the first direct measurement of this capture cross section, it should be regarded as more reliable than all previous values. It is worth pointing out that the cross-section value taken by both NIST (7.6 ± 0.8 mb) and IAEA ($8.7 \pm \text{NA}$ mb) [22,27,31], as well as the most recent values reported in the compilation by Firestone [5], underestimate the cross section measured and reported here.

$^{13}\text{C}(n, \gamma)^{14}\text{C}$. Applying Eq. (4), we obtained a cross section of 0.18 ± 0.03 b for this reaction. This value is in disagreement with the value reported in databases [22,27] (1.37 ± 0.04 mb). Clearly, our cross-section is much larger, which was evident from the large $^{14}\text{C}/^{12}\text{C}$ ratio obtained for the graphite samples (see Table II).

To verify whether it was possible to have a large contribution from higher energy neutrons to this cross section, a second irradiation with the same neutron flux (2.3×10^{13} n/cm² s at position B1) of new graphite samples enclosed in a cadmium container was performed. Cadmium absorbs neutrons with energies below ≈ 0.5 eV, therefore in this case only higher energy neutrons should contribute to the cross section. The measured cross section using cadmium as a slow neutron absorber represents only 2% of that measured without cadmium. We can conclude that the contribution of fast neutrons to our measured cross sections is very small and therefore a different explanation for the excess of ^{14}C produced in our graphite samples should exist.

The graphite samples were analyzed at the electronic microscope laboratory at IF-UNAM, using the electron-probe x-ray fluorescence (EP-XRF) analysis technique, where a contamination close to 1% of nitrogen in the material was found. Given the much larger cross section for the $^{14}\text{N}(n, p)^{14}\text{C}$ reaction (see above), compared to 1.37 ± 0.04 mb reported in databases for the $^{13}\text{C}(n, \gamma)^{14}\text{C}$ reaction [27], together

with the small concentration of target nucleus of interest ^{13}C ($R_{^{13}\text{C}/^{12}\text{C}}^0 = 0.011$), a 1% content of ^{14}N can account for the total of the ^{14}C produced in the irradiation of the graphite samples. Correcting for this contamination requires a very precise quantification of the $R_{^{14}\text{N}/^{12}\text{C}}^0$ ratio. Our estimation based on the amount of ^{14}C produced in the samples is that $R_{^{14}\text{N}/^{12}\text{C}}^0 < 8 \times 10^{-4}$. This establishes a limit on the level of purity required for the graphite samples in order to obtain a precise measurement of the $^{13}\text{C}(n, \gamma)^{14}\text{C}$ reaction cross section.

IV. CONCLUSIONS

In recent years, AMS measurements have provided data for open questions in nuclear astrophysics. In this work we developed a protocol to perform measurements of thermal neutron capture cross section using the combination of a nuclear research reactor and AMS.

We present the measurement of the thermal neutron capture cross section for the $^9\text{Be}(n, \gamma)^{10}\text{Be}$ reaction. The value we report of $\sigma = 9.7 \pm 0.53$ mb, indicates that previous publications underestimate this cross section. It is worthwhile to mention that, for this case, previous works are all indirect measurements, ours being the first direct one.

We used the $^{14}\text{N}(n, p)^{14}\text{C}$ reaction whose cross section for thermal neutrons has been measured with great accuracy as a benchmark to test the protocols we used to derive cross sections. Our measurement gave 2.07 ± 0.37 b, in agreement with previously reported values, albeit with much larger uncertainties, but still serving our purposes.

For the $^{13}\text{C}(n, \gamma)^{14}\text{C}$ reaction, the presence of a ^{14}N contamination and the impossibility of quantifying it to the required precision prevented us from obtaining the cross section. However, a limit on the content of ^{14}N in graphite of $^{14}\text{N}/^{12}\text{C} < 8 \times 10^{-4}$ was established for future experiments using this material. The use of a ^{13}C pure target, prepared by implantation of ^{13}C on an aluminium or silicon matrix, is being evaluated.

Last but not least, we showed that we can produce materials (graphite and BeO) with a well controlled enrichment in the isotopic ratio ($^{14}\text{C}/^{12}\text{C}$ and $^{10}\text{B}/^9\text{Be}$ respectively) with the potential to be produced as standards for AMS routine work.

ACKNOWLEDGMENTS

The authors would like to thank all the technical staff at IF-UNAM and ININ whose contributions made this work possible. Sergio Martínez González at LEMA and Samuel Tehuacanero Cuapa at the electron microscope facility deserve special mention for their help. We also are indebted to Javier Mas-Ruiz and Alan Omar Valdez-Guerrero for their help in the preparation of figures for the paper. This work was partly funded by CONACyT-UNAM Grants No. 271802, No. 280760, No. 280769, No. 294537, No. 299073, and No. 299186 and PAPIIT-UNAM Grants No. IG101016, No. IG100619, No. IN107820, No. IN109120, and No. AG101120. We are grateful to the continuous support by CTIC-UNAM (Coordinación de la Investigación Científica UNAM).

- [1] C. Solís, E. Chávez-Lomelí, M. E. Ortiz, A. Huerta, E. Andrade, E. Barrios, *Nucl. Instrum. Methods Phys. Res., Sect. B* **331**, 233 (2014).
- [2] G. Reza, E. Andrade, L. Acosta, B. Góngora, A. Huerta, D. J. Marín-Lámbarrí, J. Mas-Ruiz, M. E. Ortiz, S. Padilla, C. Solís, and E. Chávez, *Eur. Phys. J. Plus* **134**, 590 (2019).
- [3] The online calculators formerly known as the CRONUS-Earth online calculators, <https://hess.ess.washington.edu/> (2008).
- [4] K. De Los Ríos, C. Méndez-García, S. Padilla, C. Solís, E. Chávez, A. Huerta, and L. Acosta, *J. Phys. Conf. S.* **1078**, 012009 (2018).
- [5] R. B. Firestone and Zs. Revay, *Phys. Rev. C* **93**, 054306 (2016).
- [6] H.-Y. Zhou and Z.-H. Liu, *Chin. Phys.* **14**, 1544 (2005).
- [7] C. M. Conneely, W. V. Prestwich, and T. J. Kennett, *Nucl. Instrum. Methods Phys. Res. A* **248**, 416 (1986).
- [8] A. Wallner *et al.*, *J. Phys. G: Nucl. Part. Phys.* **35**, 014018 (2008).
- [9] S. Dubovichenko and A. Dzhazairov-Kakhramanov, *Int. J. Mod. Phys. E* **26**, 1630009 (2017).
- [10] D. D. Clayton, S. A. Colgate, and G. J. Fishman, *Astrophys. J.* **155**, 75 (1969).
- [11] D. D. Clayton and L. R. Nittler, *Annu. Rev. Astron. Astrophys.* **42**, 39 (2004).
- [12] A. Wallner *et al.*, *J. Korean Phys. Soc.* **59**, 1378 (2011).
- [13] G. R. Hennig, *Phys. Rev.* **95**, 92 (1954).
- [14] R. Reifarh *et al.*, *Phys. Rev. C* **77**, 015804 (2008).
- [15] H. Herndl, R. Hofinger, and H. Oberhummer, in *Tours Symposium on Nuclear Physics III, 2–5 September 1997, Tours*, edited by M. Arnould, M. Lewitowicz, Yu. Ts. Oganessian, M. Ohta, H. Utsunomiya, and T. Wada, AIP Conf. Proc. No. 425 (AIP, New York, 1998), p. 428.
- [16] T. Kii, T. Shima, H. Sato, T. Baba, and Y. Nagai, *Phys. Rev. C* **59**, 3397 (1999).
- [17] T. Shima *et al.*, *Nucl. Phys. A* **621**, 231 (1997).
- [18] Y. M. Gledenov, V. I. Salatski, and P. V. Sedyshev, *Z. Phys. A – Hadrons Nuclei* **346**, 307 (1993).
- [19] P. E. Koehler, *Phys. Rev. C* **48**, 439 (1993).
- [20] P. E. Koehler and H. A. O’Brien, *Phys. Rev. C* **39**, 1655 (1989).
- [21] J. Wagemans, C. Wagemans, G. Goeminne, and P. Geltenbort, *Phys. Rev. C* **61**, 064601 (2000).
- [22] S. Mughabghab, *Atlas of Neutron Resonances*, 5th ed. (Elsevier, Amsterdam, 2006).
- [23] A. Wallner *et al.*, *Phys. Rev. C* **93**, 045803 (2016).
- [24] R. Reifarh, C. Lederer, and F. Käppeler, *J. Phys. G: Nucl. Part. Phys.* **41**, 053101 (2014).
- [25] S. Merrill and W. Paul, *Astrophys. J.* **116**, 21 (1952).
- [26] E. M. Burbidge, *Rev. Mod. Phys.* **29**, (1957).
- [27] Neutron scattering lengths and cross sections. Available at <https://www.ncnr.nist.gov/resources/n-lengths/> and <https://www.oecd-nea.org/dbdata/jeff/>
- [28] J. Galicia-Aragón, J. L. François-Lacouture, and F. Aguilar-Hernandez, *Prog. Nucl. Energy* **88**, 264 (2016).
- [29] ININ, TRIGA Mark III Reactor, Safety Report of the Dr. Nabor Carrillo Flores Nuclear Center, 2014 (unpublished).
- [30] H. S. Cruz-Galindo and R. Raya-Arredondo, in *Radiation Physics: IX International Symposium on Radiation Physics, 14–17 April 2013, Puebla, Mexico*, edited by C. Vázquez-López, G. Espinosa-García, and J. Ignacio Golzarri, AIP Conf. Proc. No. 1544 (AIP, New York, 2013), p. 53.
- [31] K. Nishiizumi, M. Imamura, M. W. Caffee, J. R. Southon, R. C. Finkel, and J. McAninch, *Nucl. Instrum. Methods Phys. Res. B* **258**, 403 (2007).